AD-A152 765 COMPARISON OF VARIOUS DRAG COEFFICIENT EXPANSIONS USING POLYNOMIALS AND SPLINES(U) AIR FORCE ARMAMENT LAB EGLIN AFB FL S M SABOT ET AL. AUG 84 AFATL-85-23 1/1

UNCLASSIFIED F/G 12/1 NL

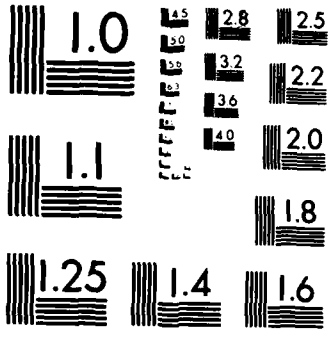

AD-A152 765

(2)

UNCLASSIFIED
SECURITY CLASSIFICATION OF THIS PAGE

REPORT DOCUMENTATION PAGE

1a. REPORT SECURITY CLASSIFICATION UNCLASSIFIED PUBLIC RELEASE	1b. RESTRICTIVE MARKINGS OPEN DISTRIBUTION
2a. SECURITY CLASSIFICATION AUTHORITY	3. DISTRIBUTION/AVAILABILITY OF REPORT for public release and sale; its distribution is unlimited.
2b. DECLASSIFICATION/DOWNGRADING SCHEDULE	
4. PERFORMING ORGANIZATION REPORT NUMBER(S)	5. MONITORING ORGANIZATION REPORT NUMBER(S) AFATL-85-23
6a. NAME OF PERFORMING ORGANIZATION AIR FORCE ARMAMENT LABORATORY AERODYNAMICS BRANCH 6b. OFFICE SYMBOL (If applicable) AFATL/DLCA	7a. NAME OF MONITORING ORGANIZATION
6c. ADDRESS (City, State and ZIP Code) EGLIN AFB FL 32542-5000	7b. ADDRESS (City, State and ZIP Code)
8a. NAME OF FUNDING/SPONSORING ORGANIZATION 8b. OFFICE SYMBOL (If applicable)	9. PROCUREMENT INSTRUMENT IDENTIFICATION NUMBER
8c. ADDRESS (City, State and ZIP Code)	10. SOURCE OF FUNDING NOS. PROGRAM ELEMENT NO.: 62602F PROJECT NO.: 2567 TASK NO.: 02 WORK UNIT NO.: 45
11. TITLE (Include Security Classification) Comparison of Various Drag Coefficient Expansions Using Polynomials and Splines	
12. PERSONAL AUTHOR(S) SABOT, SALLY M.; CHAPMAN, G.T.; and WINCHENBACH, G.L.	
13a. TYPE OF REPORT 13b. TIME COVERED FROM _____ TO _____	14. DATE OF REPORT (Yr., Mo., Day) 1984 August 15. PAGE COUNT 7
16. SUPPLEMENTARY NOTATION	
17. COSATI CODES FIELD / GROUP / SUB. GR.	18. SUBJECT TERMS (Continue on reverse if necessary and identify by block number) Aerodynamic Modeling Splines Polynomials Numerical Integration Drag Coefficients

19. ABSTRACT (Continue on reverse if necessary and identify by block number)

The longitudinal differential equation of motion has been used to investigate various aerodynamic expansion techniques. The total drag coefficient was expanded using conventional polynomials and splines with and without floating knot locations. This paper discusses the various techniques and approaches, compares results obtained from simultaneously fitting four separate flights (time vs distance measurements) and outlines the potential advantages and/or disadvantages of the various aerodynamic expansion techniques. It is believed that this is the first time splines have been used in the aerodynamic coefficient estimation process and that these results and techniques are germane to other applications.

20. DISTRIBUTION/AVAILABILITY OF ABSTRACT UNCLASSIFIED/UNLIMITED ☒ SAME AS RPT. ☐ DTIC USERS ☐	21. ABSTRACT SECURITY CLASSIFICATION
22a. NAME OF RESPONSIBLE INDIVIDUAL G. L. WINCHENBACH	22b. TELEPHONE NUMBER (Include Area Code) 904/882-4085 22c. OFFICE SYMBOL DLCA

DD FORM 1473, 83 APR EDITION OF 1 JAN 73 IS OBSOLETE.

UNCLASSIFIED
SECURITY CLASSIFICATION OF THIS PAGE

84-2113

COMPARISON OF VARIOUS DRAG COEFFICIENT EXPANSIONS USING POLYNOMIALS AND SPLINES

SALLY M. SABOT
AERODYNAMICS BRANCH
AEROMECHANICS DIVISION
AIR FORCE ARMAMENT LABORATORY
EGLIN AIR FORCE BASE, FLORIDA

G. T. CHAPMAN *
THERMO AND GAS DYNAMICS DIVISION
NASA AMES RESEARCH CENTER
MOFFETT FIELD, CALIFORNIA

G. L. WINCHENBACH *
AERODYNAMICS BRANCH
AEROMECHANICS DIVISION
AIR FORCE ARMAMENT LABORATORY
EGLIN AIR FORCE BASE, FLORIDA

ABSTRACT

The longitudinal differential equation of motion has been used to investigate various aerodynamic expansion techniques. The total drag coefficient was expanded using conventional polynomials and splines with and without floating knot locations. This paper discusses the various techniques and approaches, compares results obtained from simultaneously fitting four separate flights (time vs distance measurements) and outlines the potential advantages and/or disadvantages of the various aerodynamic expansion techniques. It is believed that this is the first time splines have been used in the aerodynamic coefficient estimation process and that these results and techniques are germane to other applications.

NOMENCLATURE

A	Reference area
a	Coefficient in Equation 3
C_i	Slopes of spline segments (see Equations 4, 5, and 6)
C_D	Total drag coefficient
C_{D_0}	Zero angle of attack drag coefficient
C_{D_2}	Second order drag term (see Equations 2 and 3)
C_{D_4}	Fourth order drag term (see Equation 3)
C_{D_V}	Drag variation due to velocity change
e	Exponential
m	Model mass
n	Number of straight line segments (see Equation 4)
RSS	Sum of residuals squared
S_i	Switches for spline segments (see Equations 4, 5, and 6)
V	Velocity along the X axis
V_i	Instantaneous velocity
V_{ref}	Reference velocity
X	Downrange axis
α_i	Instantaneous pitch angle
β_i	Instantaneous yaw angle
ξ	Total instantaneous angle of attack
ξ_i	Knot locations in Equations 4, 5, and 6
ρ	Air density

Superscripts

.	Time derivative

INTRODUCTION

Prior to 1969, the prevalent method of analyzing ballistic spark range data was based on the linear approximation method known as "linear theory" developed by Murphy[1-2] and others[3-5]. Stated briefly, the method uses a closed-form solution to the differential equations of motion. This approximate solution results from assuming a linearized aerodynamic model where the aerodynamic force and moment derivatives are constant with angle of attack (hence the name "linear theory"). Murphy extended this technique to include a quasi-nonlinear analysis[6] where the linear aerodynamic force and moment derivatives are reduced in such a manner that certain nonlinearities could be obtained. This quasi-nonlinear analysis requires an assumed functional form of the nonlinearity (normally a quadratic or cubic polynomial).

In 1969 Chapman and Kirk, in analyzing free-flight data[7], documented the application of a technique they called parametric differentiation which permitted the free flight differential equation of motion to be used directly in the

* Member AIAA

data correlation process. This technique eliminated the requirement for closed-form solutions to the equations of motion. However, it is still required to assume a form of the nonlinearities in the equations of motion. Generally these forms have also been assumed to be polynomial expansions of the aerodynamic force and moment derivatives with angle of attack[8-9].

During the past several years, data analysts have discussed the possibility of using mathematical splines (two or more mathematical expressions attached end to end) for the coefficient expansions. These splines permit the slopes of the aerodynamic expansions to be discontinuous and would offer the analyst a more general aerodynamic model, thereby relieving some of the requirements of assuming the form of the nonlinearities. This paper discusses various coefficient expansion techniques and compares results obtained using the various expansions.

METHOD OF APPROACH

In order to evaluate the various expansion techniques (continuous function vs splines), we will restrict our attention to a simple single degree of freedom system rather than the full six-degree of freedom system described in various references.[8-9]

Longitudinal Momentum Equation

This paper will examine the determination of the total drag coefficient (C_D) as a function of instantaneous angle of attack and velocity from the longitudinal momentum equation and the associated experimental measurements of distance traveled vs time. The differential equation governing the longitudinal momentum is

$$\ddot{X} = -\frac{\rho A}{2m} C_D \dot{X}^2 \qquad (1)$$

where ρ is the air density, A is the body reference area, m is the projectile mass, X is the longitudinal down range distance, and $(\dot{\ })$ and $(\ddot{\ })$ indicate the first and second derivatives with respect to time. The total drag coefficient, $C_D(\delta,V)$, depends on the instantaneous total angle of attack, $\delta = \sqrt{\sin^2\alpha + \sin^2\phi}$, and velocity, $V = \dot{X}$. Equation (1) assumes that the angle between the velocity vector and the X axis is small.

Expansions for the Total Drag Coefficient

Several expansion techniques for C_D were investigated. The first two involved continuous functions, beginning with the classical quadratic dependence on angle of attack, or

$$C_D = C_{D_0} + C_{D_2}\delta^2 \qquad (2)$$

Equation (2) represents the classical expression for which Murphy[1,2] developed a methodology of determining C_{D_0} and C_{D_2} by plotting the effective measured drag coefficients vs the mean of δ^2. A straight line through this data yields the intercept, C_{D_0}, and the slope, C_{D_2}. The second continuous function is much more versatile and is valid for a wider range of angle of attack dependence and a linear velocity dependence, that is

$$C_D = C_{D_0}\delta^{a} + C_{D_2}\delta^{b} + C_{D_4}\delta^{c} + C_{D_V}\dot{X} \qquad (3)$$

Note this expansion has five unknown coefficients, C_{D_0}, a, C_{D_2}, C_{D_4}, and C_{D_V} as do all the remaining expansion techniques considered within this paper. The δ^a term is somewhat unconventional but allows a nonzero slope at zero angle of attack. The C_{D_V} coefficient is normally small but for high drag configurations which experience large velocity decays during the flight or when time-distance data obtained from several flights (slightly different launch velocities) are simultaneously analyzed this term can be important. This C_{D_V} term accounts for variations in drag coefficients with Mach number and Reynolds number. The two effects cannot be simply separated because they both depend linearly on velocity. This term appears in all of the expansions discussed except for the classical quadratic dependence shown in Equation (2).

Several expansions using spline functions were also evaluated. The first of these uses multiple straight line segments (see Figure 1) and the general expansion is

$$C_D = C_{D_0} + \sum_{i=1}^{n} C_i S_i (\delta - \delta_i) + C_{D_V}\dot{X} \qquad (4)$$

where i is the index for the segment, δ_i's are the knot locations, C_i's are the slopes of each segment, and S_i's are the switches ($S_i = 0$ or 1 depending on whether or not the instantaneous value of δ is within the range of the segment). For the investigation discussed, the evaluations of the various expansion techniques were restricted to four unknown coefficients plus the C_{D_V} term. Hence only two cases utilizing straight line segments were considered. The first case is three segments (n=3) with the knots fixed at δ_1, and δ_2. These knot locations were chosen by dividing the δ range into three equal parts, $\delta_1 = \delta_{max}/3$, $\delta_2 = 2\delta_{max}/3$, $\delta_3 = \delta_{max}$. The five unknown coefficients then become C_{D_0}, C_1, C_2, C_3, and C_{D_V}. Here it should be noted that other methods of dividing the δ space into segments and selecting the knot locations were considered. Initially, it was felt that the segments should be chosen such that those associated with the higher angles of attack would be small compared to the segments associated with the smaller angles of attack. The reasoning for this was that it was assumed that the rate of change of the drag coefficient with respect to δ was much higher at large angles of attack thereby requiring smaller segments. Although this assumption is certainly true for most free flight range data, the nature of a well behaved dynamically stable configuration in free flight is that the larger initial angles of attack rapidly decrease (damps) during the flight. Hence only a relatively few data points

representing the initial high angles of attack are normally obtained compared with the number of data points associated with the smaller angles of attack (for example, see Figure 2). Considering this, if a small segment was chosen for the higher angles of attack, only a very few data points would fall within this segment thereby invalidating the resultant slope parameter. After this anomaly was recognized it was felt that perhaps the knot locations should be selected such that each segment contained an equal number of data points. However it immediately became obvious that due to the nature of the data, a very small segment resulted at the smaller angles of attack, where it wasn't needed, and a large segment resulted at the large angles of attack where a small segment was desired (see Figure 3). With these considerations is mind, dividing the δ range into equal parts appeared to be a reasonable compromise. However, if this technique is applied to other free flight data (i.e., dynamically unstable configurations) or to another application altogether, the logic associated with selecting the knot locations should be revisited.

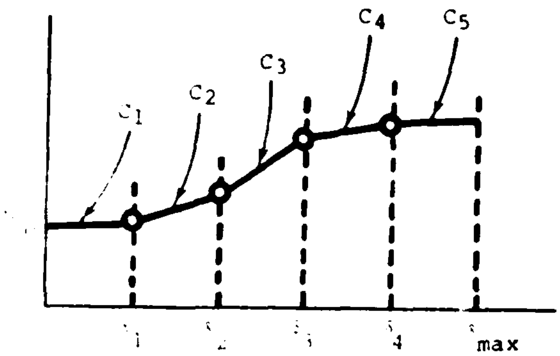

[illegible] eral multi-dimensional straight [illegible]

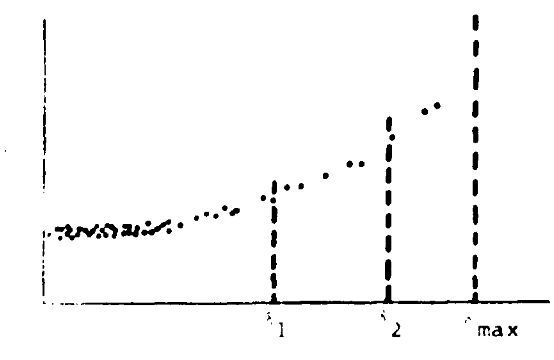

[illegible] experimental [illegible]

The second case utilizing straight line segments splined together possessed only two segments, n=2 in Equation (4), but the knot (δ_1) was allowed to be a free variable and determined by the data reduction procedure. Hence the five unknown coefficients become $C_{D_o}, C_1, C_2, \delta_1$ and C_{D_v} (see Figure 4).

Another set of splines used in the present investigation involves quadratic segments similar to Equation (2). Here, the knot locations are free variables and are determined by the data reduction routine (see Figures 5a and 5b). This expansion can be defined such that not only is the C_D function continuous at the knot, but also the derivative can be made continuous at the knot. Both of these approaches are discussed. First, consider the approach where only C_D is continuous at the floating knot location. This expansion is written as

$$C_D = C_{D_o} + S_1 C_1 \delta^2 + S_2 C_2 \delta_1^2 + [illegible]\, 2 (\delta^2 - \delta_1^2) + [illegible] (\delta - \delta_{ref}) \quad (5)$$

Here C_{D_o}, C_1, C_2, δ_1, and C_{D_v} are the five free variables and the function has a discontinuous slope at δ_1. S_1 and S_2 are the determining switches for the polynomials and are set similarly to those in Equation (4) (i.e., if $\delta^2 < \delta_1^2$ then $S_1 = 1$ and $S_2 = 0$ or if $\delta^2 > \delta_1^2$, then $S_1 = 0$ and $S_2 = 1$). This approach requires the evaluation of only one set of partial derivatives with respect to C_1 or C_2 depending on the magnitude of δ^2.

Equation (5) can be modified by adding an additional term such that the slope of the C_D vs curve is also continuous at the floating knot location to yield

$$C_D = C_{D_o} + S_1 C_1 \delta^2 + S_2 C_2 \delta_1^2 + [illegible] (C_1 - C_2)(\delta - \delta_1 [illegible]) + [illegible]\, 2\, 2 (\delta^2 - \delta_1^2) + [illegible] (\delta - \delta_{ref}) \quad (6)$$

The unknown coefficients for this expression are the same as for Equation (5), and the switches are set similarly.

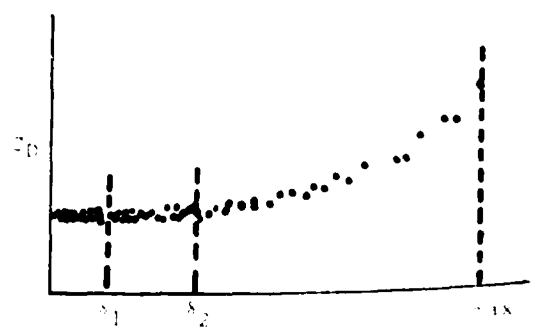

[illegible] data with [illegible]

There are many other spline expansions that could be considered using five free unknown coefficients; however, it is believed the ones defined herein are sufficient to illustrate the applicability and usefulness of these techniques.

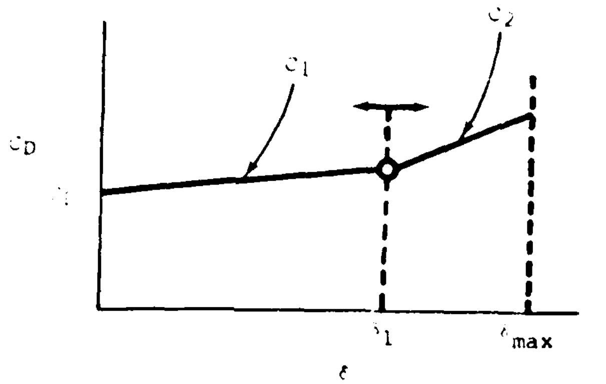

Fig. 4 Two straight line segments with floating knot location

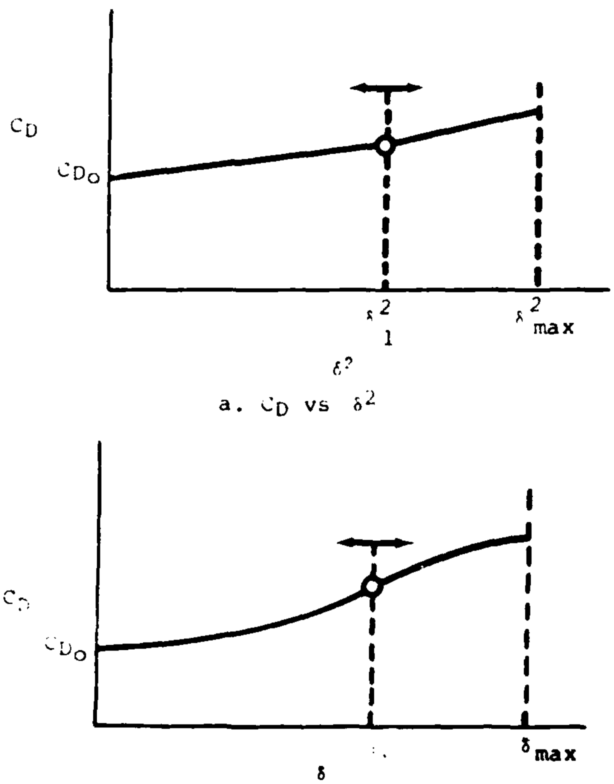

a. C_D vs δ^2

b. C_D vs δ

Fig. 5 Two quadratic segments with floating knot location

Parameter Identification

The unknown free coefficients in the various expansions Equations (2) through (6) are determined by fitting the experimentally measured time and distance data with the numerical solution of Equation (1). This fitting process is a least squares technique and the angle of attack history is provided as an input. The method used is the one described by Chapman and Kirk[7]. This method will be described briefly to illustrate the technique when spline functions are employed for expansion of the total drag coefficient. The steps utilized in applying the technique are as follows:

1. Identify/formulate the associated equation of motion. For the application discussed this has been accomplished and is Equation (1).

2. Select an appropriate expansion of the aerodynamic coefficients. This step is the subject of this paper: the investigation of several expansion techniques as defined in Equations (2) through (6).

3. Partially differentiating the equation of motion, Equation (1), with respect to each of the free unknown coefficients, form a set of parametric differential equations. This is illustrated below by using the expansion shown in Equation (5). Let

$$P_1 = \frac{\partial X}{\partial C_{D_0}}, \quad P_2 = [illegible], \quad P_3 = [illegible], \quad P_4 = [illegible],$$

$$P_5 = \frac{\partial X}{\partial C_{D_0}}, \quad P_6 = [illegible], \text{ and } P_7 = [illegible] \qquad (7)$$

Applying this to Equations (1) and (2) the following set of parametric differential equations are derived.

$$\ddot{P}_1 = -K\dot{X}^2 (1 + C_{D_0} [illegible]) - 2K\dot{X} [illegible]$$
$$\downarrow$$
$$\ddot{P}_4 = -K\dot{X}_0^2 \{2S_2(C_1\delta_1) - 2S [illegible]$$
$$\downarrow$$
$$\ddot{P}_7 = -K\dot{X}^2 \{(\ )_0 [illegible] \qquad (8)$$

where K is $\rho A/2m$ and $(\ )_0$ implies the quantity was evaluated with given coefficients (either initial guesses or corrected values) at the start of each iteration cycle.

4. Numerically integrate the equation of motion, Equation (1), utilizing initial guesses for the unknown aerodynamic coefficients and estimated initial conditions (X_e and $\dot{X}_e$). The numerical integration technique used is a Gauss-Newton iterative method.

5. Integrate parametric equations, Equations (8), numerically such that the partial derivatives with respect to each of the free unknown coefficients are evaluated.

6. The method of differential corrections is then used to obtain corrections to the initial guesses of the unknown aerodynamic coefficients

and estimated initial conditions (X_e and $\dot{X}_o$). This method consists of expanding the calculated value of position $X_{i\ cal}$ about a given set of coefficients in a Taylor series. Or

$$X_{i\ cal} = X_{ical_c} + \sum \frac{\partial X}{\partial C_j}\Big|_o \Delta C_j + \text{Higher Order Terms} \quad (9)$$

Note the subscript o again indicates calculated values using the given set of coefficients and the summation, ignoring the higher order terms, provides the contribution to $X_{i\ cal}$ associated with small changes in the coefficients (C_j's). The sum of the squares of the residuals, RSQ, (difference between measured and calculated downrange distance traveled) is given as

$$RSQ = \sum_{i=1}^{\ell} (X_{i\ meas} - X_{i\ cal})^2 \quad (10)$$

The subscript i denotes the i-th measurement and ℓ the total number of measurements. Equation (10) can accommodate the reduction/analysis of several simultaneous data sets; however, for simplicity the notation will indicate only one set of time and distance measurements (see Reference 8 for details on simultaneous fitting of multiple data sets).

Now substituting Equation (9) into Equation (10), taking the derivative of RSQ with respect to each of the unknown coefficients (C_k) and setting equal to zero, after some manipulation one can arrive at the following matrix equation,

$$C = (A_{jk})^{-1} B_k \quad (11)$$

where

$$A_{jk} = \sum_{i=1}^{\ell} \frac{\partial X}{\partial C_j} \frac{\partial X}{\partial C_k}$$

and

$$B_k = \sum_{i=1}^{\ell} (X_{i\ meas} - X_{i\ cal}) \frac{\partial X}{\partial C_k}$$

Here, C is the matrix of corrections to be added to each of the unknown coefficients to be determined including the initial conditions X_e and $\dot{X}_o$. Once the experimental data is compared to the numerically integrated position profile in a least squares sense, the corrections to the unknown coefficients and initial conditions can be determined using Equation (11).

7. Steps 3 through 6 are then repeated, using the newly adjusted coefficients and initial conditions, and the process continues until desired convergence is obtained.

RESULTS AND DISCUSSION

The estimated total drag coefficient (C_D) variations obtained using the various expansion techniques, Equations (2) through (6), are shown in Figures 6 through 8. Each of these C_D expansions were evaluated by simultaneously fitting four sets of experimentally measured time and distance data obtained from four separate flights of a 25mm spin stabilized projectile tested in the Aeroballistics Research Facility[10]. This set of data was used to evaluate the C_D expansions because of the relatively high angles of attack experienced during some of the flights and the apparent highly nonlinear characteristics of C_D with total angle of attack. The initial velocity (muzzle) varied from 3168 to 3245 ft/sec for the four flights and the average mid-range velocity (V_{REF}) of all four flights being 3098 ft/sec.

Here it should be cautioned that because some of the expansion techniques fit this particular set of data better than others, it doesn't necessarily mean that one expansion method is superior to another. In fact, the analyst should recognize that when selecting an expansion (whether it is one of the expansions discussed herein or another) for a particular application the inherent nature of the data itself should be the dominate consideration. For example, if time and position data obtained from the flight of a sphere were being analyzed (angle of attack is of no concern) the expansion would only include the C_{D_o} and C_{D_v} terms. Or, if a highly nonlinear spring-mass-damper system was being analyzed, the frequency of oscillation and/or damping may be modeled as a function of the displacement using multiple straight line segments with or without floating knots. For this case, one may possess information which identifies where the knot should be located. Also, a good rule of thumb to remember is to use the simplest expansion which adequately matches that particular set of data. With these considerations in mind, the C_D expansions using the various techniques previously discussed are presented to show the applicability and versatility of these methods. Furthermore, they graphically illustrate to any potential user that the more conventional continuous functions are not the only choices available.

Figure 6 shows the comparison of the classical quadratic (Equation 2) with the fourth order polynomial including both the $\theta\alpha^2$ and C_{D_v} terms (Equation 3). As shown in this figure, the fourth order polynomial resulted in a significantly better fit to the four separate flights than the quadratic (note sum of the residuals squared, RSQ, for both expansions). However, this should not be unexpected since the fourth order polynomial has three additional unknown coefficients (a, C_{D_4}, C_{D_v}), and this added flexibility would be expected to yield a lower RSQ. The real question here is whether or not the dramatic rise in C_D at the highest angles of attack is real. The four flights used for these comparisons had a total of 139 data points of which only four data points possessed angles of attack greater than 20 degrees. Hence the added flexibility may be providing erroneous results at the higher angles of attack. This would be especially true if one of the four data points, above 20 degrees, is in error. Normally, because of the paucity of data at the higher angles of

attack, the C_D expansions would only be presented up to about 20 degrees. But for the purpose of this paper, the expansions are shown up to the maximum angle of attack.

It is also of interest to see the effect of the various terms in the fourth order polynomial, Equation (1). Table 1 presents the results obtained from running five different cases with various terms held at zero in the fourth order polynomial. Case 1 shown in this table represents the classical quadratic as plotted in Figure 6.

TABLE 1

[illegible] POLYNOMIAL TERMS

	Case 1	Case 2	Case 3	Case 4	Case 5
C_{D_0}	.31	0.32	0.31	0.32	0.30
C_{D_2}	7.65	7.22	8.89	5.05	-1.17
C_{D_4}	0	0	14.68	0	35.18
a			0	0.14	2.25
C_{D_V}	0	-0.11	-0.11	-0.09	-0.12
RSQ, ft^2	.11	0.11	0.07	0.10	0.02

Case 5 represents the complete fourth order polynomial expansion, also shown in Figure 6. Cases 2 through 4 represent the results obtained when the remaining three unknown coefficients, C_{D_V}, C_{D_4}, and a, are included in the reduction routine. When viewing the results shown in Table 1, it is apparent that the C_{D_V} term is important for this particular set of data (note RSQ for Case 2 compared with Case 1) and appears to be consistently determined for all cases. What is remarkable about the results shown in this table is the dramatic improvement in the overall quality of fit (lower RSQ) when all of the unknown coefficients are determined simultaneously (see Case 5). This indicates that this particular set of time-position data requires a relatively complex expansion of C_D with angle of attack and velocity.

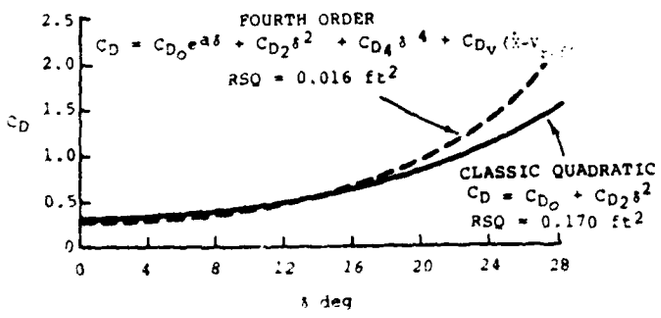

Fig. 6 Comparison of classic quadratic and fourth order expansions

The comparison of the three segment linear spline, Equation (4) with n=3, containing fixed knot locations to the two segment linear spline (also Equation 4 with n=2) containing a floating knot location is shown in Figure 7. This figure illustrates that the fit containing three segments is superior to the two segments fitted with the floating knot (note RSQ for both fits). This result is not to be unexpected since the quality of fit should improve by increasing the number of segments. What is interesting is that the sum of the residual squared for the three segment case is the same as the fourth order polynomial shown in Figure 6 (RSQ = [illegible] for both). It is suspected that this is a result of the fortuitous knot location (arbitrarily set by dividing the δ space into three equal segments) at 18.3 degrees.

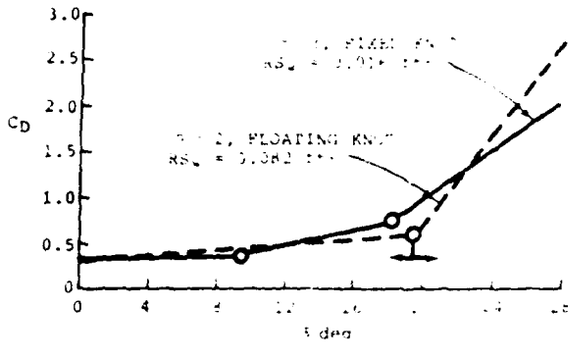

Fig. 7 Comparison of two [illegible] segment fits (see Equation 4)

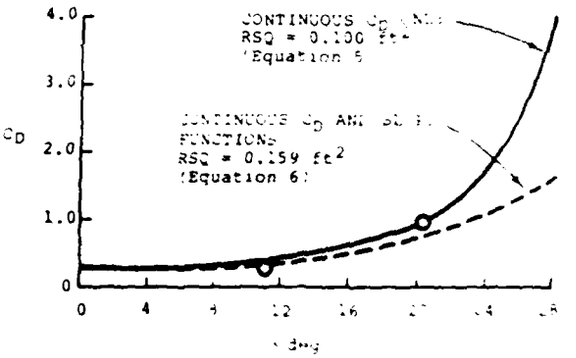

a. Quadratic splines plotted [illegible]

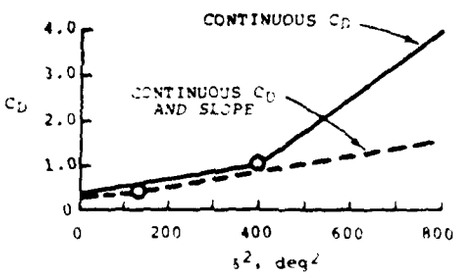

b. Quadratic splines plotted vs

Fig. 8 Comparison of quadratic splines with continuous and discontinuous slopes

The quadratic splines with a continuous C_D expansion only (Equation 5) and a continuous C_D and slope expansion (Equation 6) are compared in Figure 8. Part a of this figure shows both expansions plotted against ξ; whereas, Part b shows the expansions plotted vs ξ^2. Neither of these expansions resulted in a fit to the chosen set of data as well as the fourth order polynomial or the three segment linear spline.

Both of these expansions also contain a condition in which the coefficient extraction technique becomes indeterminate. This condition exists when the user permits the knot location to be a free variable and the slope of the first segment is nearly equal to the slope of the second segment ($C_1 \approx C_2$). When this occurs, the minimum RSQ is insensitive to the location of the knot and the iteration process fails to converge. However, if it is recognized that this condition exists, the knot location can be held constant and the iterative process again becomes stable. This condition is also indicative of an overly defined system. For instance, a single quadratic expansion would fit the data as well as the two quadratic expansions splined together. It seems for the set of data used, neither quadratic expansion appears to be advantageous. Nevertheless, this technique does appear to hold promise for modeling other aerodynamic coefficients which are highly nonlinear such as magnus terms.

CONCLUSIONS

Various total drag coefficient expansions using polynomials and/or splines have been developed and compared. A set of four flights was selected to show the applicability and versatility of these methods.

All of the expansions provided a better fit to the experimental data than the classic linear theory suggesting the need for a relatively complex expansion of C_D with angle of attack and velocity. The fourth order polynomial and the three segment spline provided superior fits. However, these results are unique for this particular data set and do not imply that they are the best expansions to use in every case.

These techniques as applied in the aerodynamic coefficient estimation process show great potential for other highly nonlinear applications. Moreover, they demonstrate that conventional, continuous functions are not the only choices available to the data analyst.

ACKNOWLEDGEMENTS

The authors wish to acknowledge the contributions of Mr. Fran Loper and Mr. C. J. Welsh, Arnold Engineering Development Center (AEDC), Tullahoma, TN to the development of the original drag program used and modified for this investigation. This program was written over a decade ago when Mr. Winchenbach was also at AEDC and has been used several times over the years to experiment with various modeling techniques. Some of these modeling experiments are described in this paper. Lt. Randy Buff (USAF) of the Air Force Armament Laboratory (AFATL) also deserves recognition for his assistance in accomplishing many of the program modifications required during this investigation.

REFERENCES

1. Murphy, C. H., "Data Reduction for Free Flight Spark Ranges", Ballistic Research Lab., Aberdeen Proving Ground, Rept. 900, February 1954.

2. Murphy, C. H., "Free Flight Motion of Symmetric Missiles", Ballistic Research Lab., Aberdeen Proving Ground, Rept. 1216, July 1963.

3. Nicolaides, J. D., "Free Flight Dynamics", University of Notre Dame, South Bend, Indiana, 1967.

4. Nicolaides, J. D., "On the Free Flight Motions of Missiles Having Slight Configurational Asymmetrics", Ballistic Research Lab., Aberdeen Proving Ground, Rept. 858, June 1953.

5. Eikenberry, R. S., "Analysis of the Angular Motion of Missiles", Sandia Rept. SC-CR-70-6051, February 1970.

6. Murphy, C. H., "The Measurement of Non-Linear Forces and Moments by Means of Free Flight Tests", Ballistic Research Lab., Aberdeen Proving Ground, Rept. 974, February 1956.

7. Chapman, G. T., and Kirk, D. B., "A Method for Extracting Aerodynamic Coefficients from Free Flight Data", AIAA Journal, Vol. 8, April 1970, pp. 753-757.

8. Whyte, R. H., Winchenbach, G. L., and Hathaway, W. H., "Subsonic Free-Flight Data for a Complex Asymmetric Missile", Journal of Guidance and Control, Vol. 4, Number 1, Jan-Feb 1981, pp. 59-65.

9. Winchenbach, G. L., Uselton, B. L., Hathaway, W. H., and Chelekis, R. M., "Comparison of Free-Flight and Wind Tunnel Data for a Generic Fighter Configuration," Journal of Aircraft, Vol. 21, Number 1, January 1984, pp. 5-13.

10. Winchenbach, G. L., Galanos, D. G., Kleist, J. S., and Lucas, B. F., "Description and Capabilities of the Aeroballistic Research Facility," AFATL-TR-78-14, April 1978

END

FILMED

5-85

DTIC